Inorg. Chem. **2006**, *45*, 6944–6949

Solvent-Controlled Synthesis and Electrochemical Lithium Storage of One-Dimensional TiO_2 Nanostructures

Qiang Wang,[†,‡] Zhenhai Wen,[†] and Jinghong Li*[,†]

Department of Chemistry, Tsinghua University, Beijing 100084, China, and Department of Chemistry, University of Science and Technology of China, Hefei 230026, China

Received March 21, 2006

In this paper, one-dimensional (1-D) nanostructured TiO_2 of different morphologies and structures have been selectively synthesized via a convenient, low-temperature solvothermal route and following calcination. Transmission electron microscopy, selected area electron diffraction, X-ray diffraction, and Brunauer–Emmett–Teller methods were used to characterize the morphology, crystalline structure, and specific surface area of these nanostructured TiO_2. The formation of different morphologies, including nanowires and nanotubes, was achieved through a deliberate control of the cosolvent. In addition to the solvent-controlled procedures, another important feature of the synthesis in the present study was that either single-crystalline nanowires (TiO_2–B) or polycrystalline nanotubes (anatase and TiO_2–B) were achieved by heat treatment at 350 °C. The electrochemical performances of the nanowires and nanotubes were further explored in terms of their potential application as anode materials for lithium-ion batteries. The lithium-insertion reactions involved in the two materials were elucidated by means of a galvanostatic method, cyclic voltammetry, and electrochemical impedance spectroscopy. The results suggest that both the crystalline structure and the unique 1-D morphology might be responsible for their favorable electrochemical properties. This work will be valuable for the understanding of the formation of nanostructured TiO_2 by the wet-chemistry process and further applications.

Introduction

In the 21st century, one of the great challenges is undoubtedly energy storage. Therefore, it is essential to seek new materials concepts to satisfy the increasing demands for energy conversion and storage worldwide.[1] Nanostructured materials might be attractive for energy devices because they combine the basic properties and unique features that arise from their nanoscale structures.[2] To realize these promising high-performance applications, the control of the physicochemical properties through their nanoscale structures is a sizable challenge.[3]

Recently, one-dimensional nanostructured TiO_2 such as nanotubes and nanowires have attracted intensive research interests because of their size- and dimensionality-dependent physicochemical properties and potential applications in the fields of solar-energy conversion, lithium batteries, and supercapacitors.[4−11] Because the synthesis of one-dimensional nanostructured TiO_2 is very important for understanding its fundamental properties, considerable effort has recently been concentrated on exploring the various synthetic methods ranging from vapor-phase techniques to solution-growth processes.[12−20] In particular, it has been found that the reaction between different TiO_2 precursors and a concentrated

* Author to whom correspondence should be addressed. Tel.: +86 10 62795290. Fax: +86 10 62771149. E-mail address: jhli@mail.tsinghua.edu.cn.
† Tsinghua University.
‡ University of Science and Technology of China.

(1) Arico, A. S.; Bruce, P.; Scrosati, B.; Tarascon, J.-M.; Schalkwijk, W. V. *Nat. Mater.* **2005**, *4*, 366.
(2) Zhang, B.; Dai, W.; Ye, X. C.; Hou, W. Y.; Xie, Y. *J. Phys. Chem. B* **2005**, *109*, 22830.
(3) Jamnik, J.; Maier, J. *Phys. Chem. Chem. Phys.* **2003**, *5*, 5215.
(4) Adachi, M.; Murata, Y.; Takao, J.; Jiu, J.; Sakamoto, M.; Wang, F. *J. Am. Chem. Soc.* **2004**, *126*, 14943.
(5) Joo, J.; Kwon, S. G.; Yu, T.; Cho, M.; Lee, J.; Yoon, J.; Hyeon, T. *J. Phys. Chem. B* **2005**, *109*, 15297.
(6) Zhou, Y. K.; Cao, L.; Zhang, F. B.; He, B. L.; Li, H. L. *J. Electrochem. Soc.* **2003**, *150*, A1246.
(7) Kavan, L.; Kalbac, M.; Zukalova, M.; Exnar, I.; Lorenzen, V.; Nesper, R.; Graetzel, M. *Chem. Mater.* **2004**, *16*, 477.
(8) Zukalova, M.; Kalbac, M.; Kavan, L.; Exnar, I.; Graetzel, M. *Chem. Mater.* **2005**, *17*, 1248.
(9) Armstrong, A. R.; Armstrong, G.; Canales, J.; Garcia, R.; Bruce, P. G. *Adv. Mater.* **2005**, *17*, 862.
(10) Armstrong, A. R.; Armstrong, G.; Canales, J.; Bruce, P. G. *Angew. Chem., Int. Ed.* **2004**, *43*, 2286.
(11) Gao, X.; Zhu, H.; Pan, G.; Ye, S.; Lan, Y.; Wu, F.; Song, D. *J. Phys. Chem. B* **2004**, *108*, 2868.
(12) Wu, J.-J.; Yu, C.-C. *J. Phys. Chem. B* **2004**, *108*, 3377.

10.1021/ic060477x CCC: $33.50
Published on Web 07/20/2006

NaOH solution under moderate hydrothermal conditions is an effective approach to prepare nanotubes and nanowires based on titania.[21,22] However, the main attention is often directed toward control over the structure and morphology only by varying the reaction temperature and reaction time during hydrothermal treatment, while an important experimental parameter, the solvent, has rarely been deliberately controlled to achieve different one-dimensional nanostructures. In the present study, we have investigated the formation of TiO_2 nanowires and nanotubes on the basis of a simple solvothermal route, which provides an opportunity for selecting the TiO_2 products with the desired morphologies and structures through a control of the cosolvent. The present method offers flexibility, selectivity, and efficiency and aims at comprehensively understanding the general reaction between concentrated NaOH and TiO_2 precursors.

It is generally accepted that breakthroughs in materials hold the key to new generations of rechargeable lithium batteries, not only for applications in consumer electronics but especially for clean energy storage and use in hybrid electric vehicles.[1] There are several potential advantages related to the development of nanomaterials for lithium-ion batteries, namely, additional reactive sites for lithium ions to produce a high specific capacity, suppression of structural changes to achieve good reversibility and cycling stability, and short path lengths for electronic and lithium ion transport to obtain a good rate capability.[3] Within this context, by investigating the lithium-insertion reactions of TiO_2 nanowires and nanotubes with various techniques including the galvanostatic method, cyclic voltammetry (CV), and electrochemical impedance spectroscopy (EIS), we are able to address the relationship between their nanoscale structures and electrochemical properties. This is of notable significance for understanding the unique properties that result from their nanoscale structure and designing new nanostructures of advanced functions.

Experimental Section

Synthesis. TiO_2 nanowires and nanotubes were synthesized by dispersing 2 g of TiO_2 (Degussa P25, which consists of about 30% rutile and 70% anatase and has a particle size of about 20 nm) in a 60 mL mixed solvent of 10 M NaOH aqueous solution and ethanol (or glycerol); the volume ratio of NaOH aqueous solution to the organic reagent was 1:1. After stirring for 1 h, the resulting suspension was transferred into a Teflon-lined stainless-steel autoclave. The autoclave was maintained at 180 °C for 18 h and then cooled to room temperature naturally. The resulting white precipitate was recovered by centrifugation and washed with a 0.1 M HCl solution and deionized water several times until the pH was 7, and the precipitate finally was calcinated at 350 °C for 4 h in the air.

Characterization. Power X-ray diffraction (XRD) was performed on a Bruker D8-Advance X-ray powder diffractometer with monochromatized Cu Kα radiation ($\lambda = 1.5418$ Å). The 2θ range used in the measurements was from 10 to 70°. Transmission electron microscopy (TEM) images were taken with a Hitachi model H-800 transmission electron microscope using an accelerating voltage of 200 kV. The structure and composition of the nanostructures were measured by high-resolution transmission electron microscopy (HRTEM; JEOL-2010F). Specific surface areas were measured by Brunauer−Emmett−Teller (BET) nitrogen adsorption−desorption (Shimadzu, Micromeritics ASAP 2010 Instrument), and pore-size distributions were calculated from the desorption branch of the N_2 adsorption isotherm using the Barrett−Joyner−Halenda (BJH) formula.

Electrochemical Measurements. Galvanostatic discharge−charge measurements were carried out using two-electrode cells with lithium metal as the counter electrode. CV and EIS measurements were carried out using three-electrode cells with lithium metal as the counter and reference electrodes. The working electrodes were fabricated by compressing the mixture of 80 wt % active materials, 10 wt % acetylene black, and 10 wt % polytetrafluoroethylene onto an aluminum foil. The pellets of the same mass were selected and then assembled as lithium batteries in an Ar-filled Labconco glovebox. The electrolyte solution was 1 M $LiPF_6$ dissolved in a mixture of ethylene carbonate (EC), dimethyl carbonate (DMC), and diethyl carbonate (DEC) with the volume ratio of EC/DMC/DEC = 1:1:1. CVs were recorded from 2.5 and 1 V at a scan rate of 0.05 mV/s, using a CHI 802B electrochemical workstation (CHI Inc., U. S. A.). Discharge−charge curves were recorded from 3 and 1 V at a current density of 110 mA/g using a Roofer Battery Tester (Shenzhen, China). Electrochemical impedance measurements were carried out on a PARSTAT 2273 Potentiostat/Galvanostat (Advanced Measurement Technology Inc., U. S. A.). The Nyquist plots were recorded potentiostatically by applying an AC voltage of 5 mV amplitude in the 100 kHz to 10 mHz frequency range. All electrochemical measurements were carried out at room temperature.

Results and Discussion

In this study, we have demonstrated a solvothermal method; by controlling the reaction between the TiO_2 precursor and concentrated NaOH solution using different organic cosolvents followed by acid washing and heating at 350 °C, well-crystallized TiO_2 nanowires and nanotubes were successfully synthesized. Figure 1 shows the different magnification TEM images of these TiO2 nanostructures. When ethanol was used as a cosolvent, on the basis of the TEM characterization, we obtained TiO_2 nanowires with diameters of about 20−50 nm and lengths of up to several micrometers (Figure 1A and B). It should be noted that some broomlike morphology has been observed. Figure 1B shows a bundle of nanowires splitting from the same root, which is a piece of crystalline sheet. When ethanol was replaced with glycerol and other conditions were kept unchanged, open-ended TiO_2 nanotubes were formed. TEM observation

(13) Armstrong, A. R.; Armstrong, G.; Canales, J.; Bruce, P. G. *Chem. Commun.* **2005**, *19*, 2454.
(14) Cozzoli, P. D.; Kornowski, A.; Weller, H. *J. Am. Chem. Soc.* **2003**, *125*, 14539.
(15) Miao, Z.; Xu, D.; Ouyang, J.; Guo, G.; Zhao, X.; Tang, Y. *Nano Lett.* **2002**, *2*, 717.
(16) Liu, S. M.; Gan, L. M.; Liu, L. H.; Zhang, W. D.; Zeng, H. C. *Chem. Mater.* **2002**, *14*, 2427.
(17) Tian, Z. R.; Voigt, J. A.; Liu, J.; Mckenzie, B.; Xu, H. *J. Am. Chem. Soc.* **2003**, *125*, 12384.
(18) Jung, J. H.; Kobayashi, H.; van Bommel, K. J. C.; Shinkai, S.; Shimizu, T. *Chem. Mater.* **2002**, *14*, 1445.
(19) Wen, B.; Liu, C.; Liu, Y. *Chem. Lett.* **2005**, *34*, 396.
(20) Wen, B.; Liu, C.; Liu, Y. *New J. Chem.* **2005**, *29*, 969.
(21) Koleńko, Y. V.; Kovnir, K. A.; Gavrilov, A. I.; Garshev, A. V.; Frantti, J.; Lebedev, O. I.; Churagulov, B. R.; Van Tendeloo, G.; Yoshimura, M. *J. Phys. Chem. B* **2006**, *110*, 4030.
(22) Lan, Y.; Gao, X. P.; Zhu, H. Y.; Zheng, Z. F.; Yan, T. Y.; Wu, F.; Ringer, S. P.; Song, D. Y. *Adv. Funct. Mater.* **2005**, *15*, 1310.

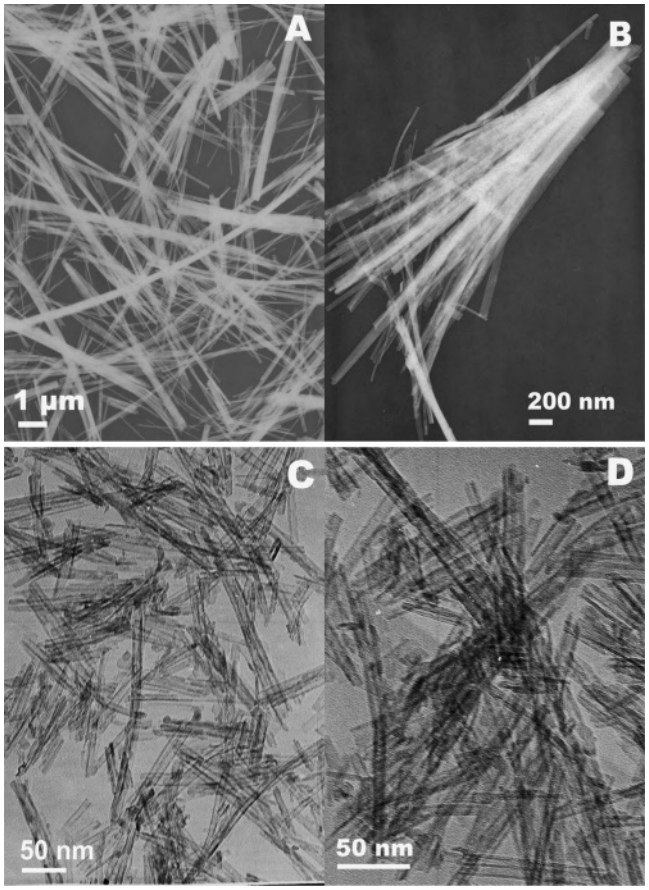

Figure 1. TEM images at different magnifications of TiO_2 nanowires (A and B) and nanotubes (C and D).

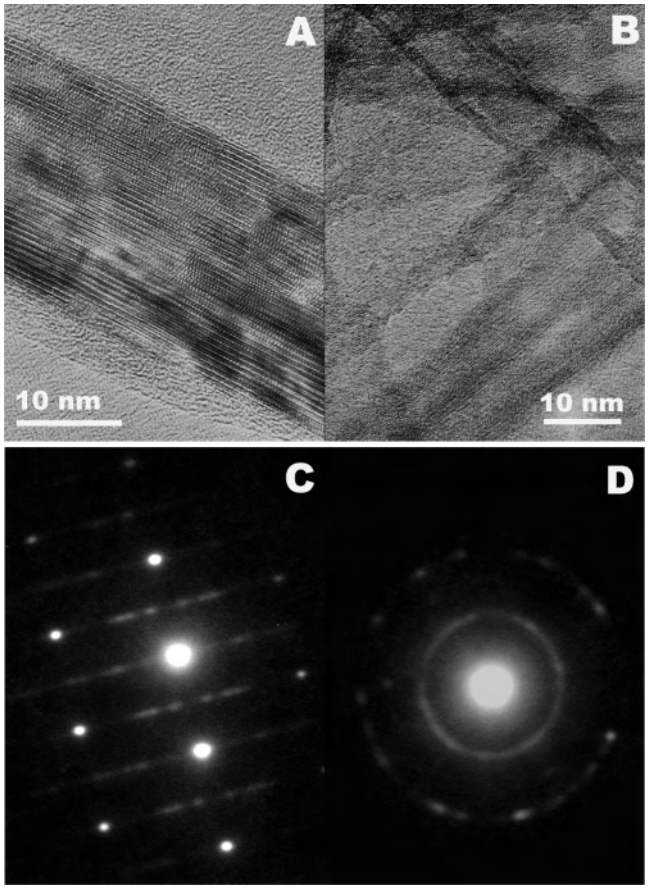

Figure 2. HRTEM images of TiO_2 nanowires (A) and nanotubes (B). Electron diffraction patterns of a single TiO_2 nanowire (C) and nanotube (D).

(Figure 1C and D) finds that the nanotubes have an inner diameter of about 8 nm, an outer diameter of about 10 nm, and a length of about 100−150 nm. A HRTEM and selected area electron diffraction investigation provides further insight into the fine microstructure and crystallinity of the products (Figure 2). A typical HRTEM image recorded from a single nanowire in Figure 2A shows a well-crystallized structure with lattice fringes of about 0.65 nm, corresponding to an interplanar spacing of TiO_2−B. The corresponding electron diffraction (ED) pattern (Figure 2C) can be completely indexed in the monoclinic *C*2/*m* space group, using the bulk TiO_2−B unit cell parameters with $a = 1.217\,87$ nm, $b = 0.374\,12$ nm, $c = 0.652\,49$ nm, and $\beta = 107.054°$.[8] The superlattice reflections confirm that the nanowires grew preferentially along the [001] direction. The HRTEM image shown in Figure 2B reveals that the nanotubes consist of continuous bilayers or multilayers; this indicates that the nanotubes may probably be formed by scrolling conjoined multilayer nanosheets.[22] The wall thickness of these nanotubes is about 2.5−3 nm; this value is in agreement with earlier reports.[13] The corresponding ED pattern taken from a single nanotube is shown in Figure 2D. It is characteristic of a tubular structure exhibiting (101) and (200) diffractions of the anatase main phase. The composition of the nanostructures was characterized by energy-dispersive X-ray spectroscopy; the results showed that the molar ratio of Ti to O in the products is around 1:2 (the spectrum is not shown). At this stage, we do not have more details to

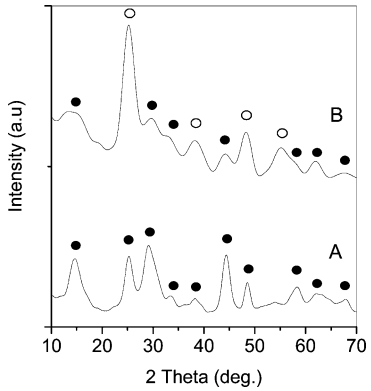

Figure 3. XRD patterns of TiO_2 nanowires (A) and nanotubes (B). Solid circles: TiO_2−B. Hollow circles: anatase.

elucidate the formation mechanism of the nanowires and nanotubes unambiguously. However, this work presents evidence that they can be obtained selectively by the tuning of cosolvents. A possible reason for this phenomenon is that the polarity and coordinating ability of a cosolvent have a strong effect on the solubility, reactivity, and diffusion behavior of the reactants, thus ultimately influencing the structure and morphological features of the resulting products.[20]

Figure 3 shows the XRD patterns of TiO_2 nanowires and nanotubes. The broadening of their diffraction peaks is due to dimensional confinement as compared to that of their bulk

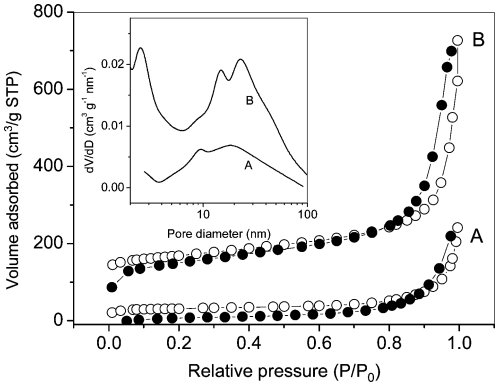

Figure 4. N_2 adsorption and desorption isotherms of TiO_2 nanowires (A) and nanotubes (B). The volume adsorbed of A is multiplied by a factor of 5. Solid circles: adsorption. Hollow circles: desorption. The inset shows BJH pore-size distributions of the two nanocrystallines.

counterparts.[9] All diffraction peaks of TiO_2 nanowires (Figure 3A) can be indexed as TiO_2−B characterized by corrugated sheets of corner- and edge-sharing TiO_6 octahedra linked together by bridging oxygen atoms.[10] On the basis of an overlap of the main characteristic diffraction peaks, TiO_2 nanotubes (Figure 3B) are dominated by the anatase phase, in which TiO_6 octahedra share two adjacent edges in the *ac* and *bc* planes,[23] with a coexistent TiO_2−B phase. The formation of TiO_2−B in TiO_2 nanotubes is not surprising, because the employed calcination temperature is not high enough to recrystallize intermediate TiO_2−B into anatase. As was known, annealing at over 400 °C of acid-washed nanotubes would result in a loss of the tubular morphology. In contrast, acid-washed nanowires convert to metastable TiO_2−B while maintaining their cylindrical morphology upon heating.[10] Thus, in this work, 350 °C was chosen as the calcination temperature in order to remove water and retain the original morphology of the nanotubes, although a coexistent TiO_2−B phase was observed.

The nitrogen adsorption/desorption isotherms at 77 K and pore-size distributions of TiO_2 nanowires and nanotubes are presented in Figure 4. When the absence of nitrogen adsorption at very low pressure is considered, it can be concluded that the micropore contribution to the total pore volume was negligible for the two materials. As seen from Figure 4B, the adsorption curve gradually increased in the middle-pressure region and exhibited an abrupt increase in the high-pressure region (>0.8 P/P_0), so the adsorption behavior of TiO_2 nanotubes can be attributed to the capillary condensation and multilayer adsorption of nitrogen in the mesopores or macropores.[24] As for TiO_2 nanowires (Figure 4A), reasonably, they exhibited the adsorption characteristics of nonporous or macroporous materials. These conclusions can be seen as in good agreement with BJH pore-size distributions of TiO_2 nanowires and nanotubes. The values of the BET surface area can be as high as 148.2 m^2/g for the latter and about 17.8 m^2/g for the former.

Figure 5 displays the initial two cyclic voltammograms and discharge−charge curves of TiO_2 nanowires and nanotubes. It can be seen that the electrochemical properties of the two materials are quite different. For TiO_2 nanowires (Figure 5A1), we observed a pair of broad cathodic/anodic peaks centered at 1.55 and 1.71 V with poorly defined shoulders. As expected, it exhibited a small irreversible capacity and relatively little difference between the first and second cycles. This phenomenon could be explained by the fact that TiO_2 nanowires have freely accessible parallel channels, which follow the [001] direction, in which lithium ions can be accommodated without any remarkable distortion of the structure.[8] The lithium-insertion characteristic could be corroborated by the corresponding discharge−charge curves (Figure 5A2) that exhibited almost monotonic voltage evolution without a constant potential region. The small sizes and dimensional confinement of TiO_2 nanostructures may result in changes in the Li-insertion energetics and, hence, smooth the discharge−charge curves. Such changes in energetics could originate from the contribution of surface free energy to the overall Li-insertion process as well as differences in the structural strains associated with lithium insertion/removal or differences in Li^+/e^- ordering, compared with those of bulk counterparts.[25] TiO_2 nanotubes (Figure 5B1), by contrast, demonstrated multiple cathodic/anodic peaks. The 1.68 and 2.02 V well-resolved peaks were associated with lithium insertion/extraction in the anatase lattice. However, the extra poorly defined and overlapping peaks were not yet clearly expounded. In view of the XRD result (see above), we suppose that they are signatures of the Li-insertion behavior of the TiO_2−B structure. As a consequence, TiO_2 nanotubes accommodated lithium ions through not only the anatase lattice but also the TiO_2−B structure, with the former embedded in a matrix of the latter. Correspondingly, the single voltage region for the anatase evolved toward progressive discrete different potentials for the TiO_2−B in its discharge curves (Figure 5B2), which represented two different lithium-insertion mechanisms in TiO_2 nanotubes. A comparative theoretical study of Li insertion into TiO_2−B and anatase points at beneficial properties of the former. As a result of lithium insertion, weak Ti−Ti bonding interactions are formed in both compounds. Crystal orbital calculations show that a small distortion of the anatase framework is required to achieve Ti−Ti bonds, whereas such a distortion is not necessary in TiO_2−B.[23] Therefore, it is natural to assume that Li^+ insertion into nanometer-sized TiO_2−B is primarily not a kinetic process but that lithium storage in anatase appears to be thermodynamically favorable, which is controlled by the solid-state diffusion of Li^+.[7] As shown in Figure 5, TiO_2 nanotubes exhibited a remarkably higher initial discharge capacity than that of TiO_2 nanowires (230 mA h/g), up to 335 mA h/g, which is near the stoichiometry Li/Ti = 1. It should be mentioned that lithium surface storage at reduced nanometer-sized particles can indeed be energetically favored; hence, the charge storage at the surface may also contribute to a remarkably high Li-storage capacity, especially in the case of the nanotubes which exhibit a significantly high surface area. Another important feature of the discharge−charge curves of TiO_2 nanostructures is the

(23) Nuspl, G.; Yoshizawa, K.; Yamabe, T. *J. Mater. Chem.* **1997**, *7*, 2529.
(24) Li, F. X.; Wang, Y.; Wang, D. Z.; Wei, F. *Carbon* **2004**, *42*, 2375.
(25) Armstrong, A. R.; Armstrong, G.; Canales, J.; Bruce, P. G. *Electrochem. Solid-State Lett.* **2006**, *9*, A139.

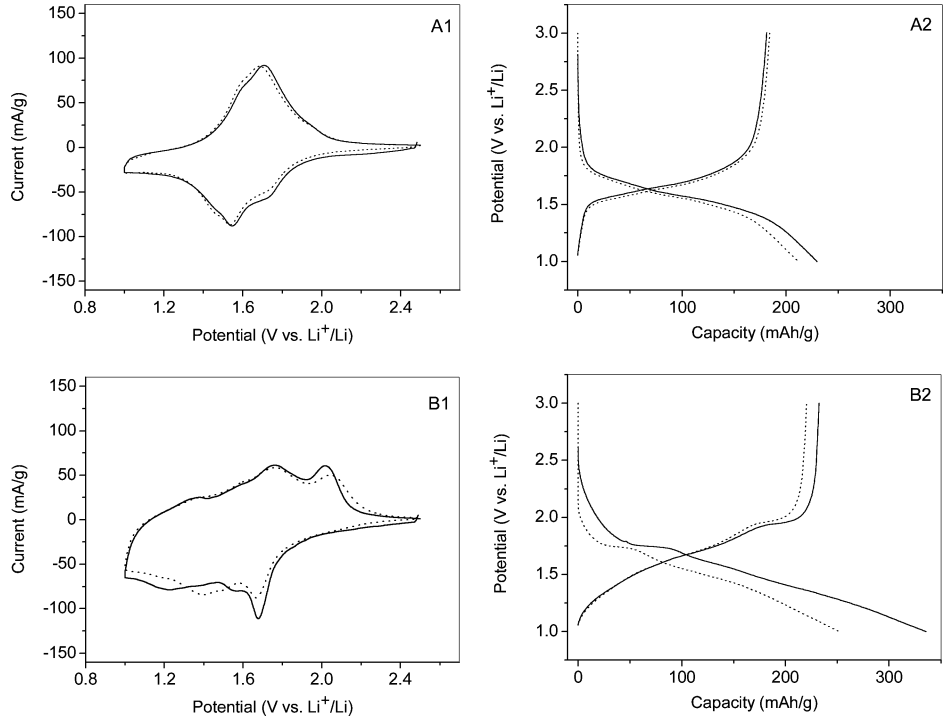

Figure 5. Initial two cyclic voltammograms (A1 and B1) at a scan rate of 0.05 mV/s and discharge−charge curves (A2 and B2) at a current density of 35 mA/g of TiO_2 nanowires (A) and nanotubes (B). Full lines: the first cycle. Dashed lines: the second cycle.

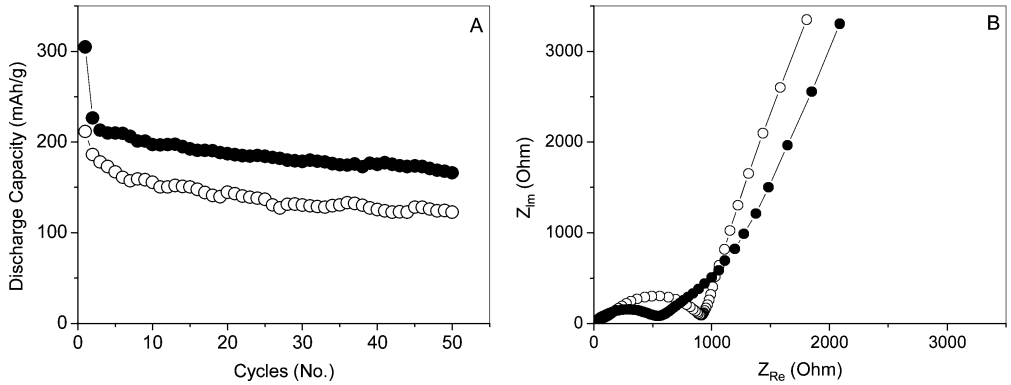

Figure 6. (A) Variation of the discharge capacity with the number of cycles for TiO_2 nanowires and nanotubes at a current density of 110 mA/g. (B) Nyquist plots at open-circuit voltage of TiO_2 nanowires and nanotubes before cycling. Hollow circles: TiO_2 nanowires. Solid circles: TiO_2 nanotubes.

existence of an irreversible capacity in the first cycle. In contrast to the behavior of the nanowires, there is significant irreversibility in the case of the nanotubes owing to a larger surface area, where only around 232 mA h/g of the 335 mA h/g of the charge inserted can be removed. It is likely that there are two reasons to account for a higher irreversible capacity loss for TiO_2 nanotubes. One is due to its anatase structure, in which the connection between TiO_6 octahedra is seriously distorted in contrast to the lithium insertion in TiO_2−B, and this is a principal difference of the lithium insertion in the both frameworks.[23] The other is due to increasingly significant surface defects such as surface vacancies or voids, which is most likely connected to some structural changes after lithium insertion and, furthermore, results in a certain fraction of lithium ions being trapped in the imperfection of the surface structure.[11]

Figure 6A presents the cycling performance of TiO_2 nanowires and nanotubes at a current density of 110 mA/g. For TiO_2 nanotubes (solid circles), their initial discharge capacity exceeded 300 mA h/g. After a significant capacity drop in the second cycle, they presented favorable cycling capability during the subsequent charge/discharge. From the 2nd to the 50th cycle, the average capacity loss was less than 1.25 mA h/g per cycle. For TiO_2 nanowires (hollow circles), they delivered a first discharge capacity of 212 mA h/g and a good capacity retention corresponding to an average capacity loss of 1.29 mA h/g per cycle. In conclusion, the TiO_2 nanowires and nanotubes may lighten the structural strains of lithium insertion/removal during the numerous charge−discharge cycles, and then, the irreversible phase transitions in response to these strains are partially suppressed. The Nyquist plots at an open-circuit voltage of TiO_2 nanowires and nanotubes are shown in Figure 6B. There is no evidence for a significant surface layer formation on the TiO_2 surface presumably because the potential is maintained above 1 V. As for TiO_2 nanowires (hollow circles), a well-defined semicircle at high frequencies and a near-vertical straight line at low frequencies were observed, corresponding

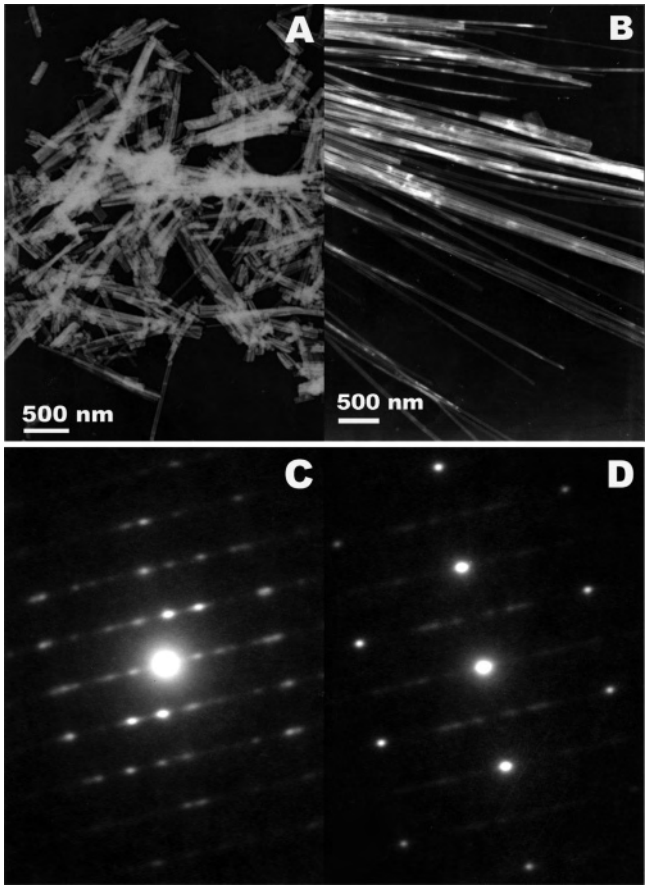

Figure 7. TEM images of TiO_2 nanosheets (A) and nanowires (B). Electron diffraction patterns of a single TiO_2 nanosheet (C) and nanowire (D).

respectively to the charge-transfer resistance associated with the surface properties of insertion materials and the solid-state diffusion resistance of lithium ions within the host.[26] This blocking-electrode-type behavior in the lower-frequency region is due to the limited diffusion of lithium ions.[27] As for TiO_2 nanotubes (solid circles), their charge-transfer resistance value in the high-frequency range was remarkably lower than that for TiO_2 nanowires; this may be interpreted as resulting from their significantly high specific surface area and hollow-inside tubular structure, which contributes to an increase in the electrode/electrolyte contact area and facilitates the charge-transfer process occurring at both the outer and inner sides of the tube walls, thus leading to a lower resistance value. Furthermore, their intermediate-frequency response was characterized by a straight line inclined at an angle of around 45° corresponding to the semi-infinite diffusion process, and at very low frequencies, a near-vertical line associated with the finite diffusion process was observed. By comparing the EIS spectra in Figure 6B, it can be concluded that the differences between the Nyquist plots exhibited by TiO_2 nanowires and nanotubes, in turn, were reflected by the differences between their lithium-insertion mechanisms.

Depending on its outstanding chemicophysical properties and extensive applications, TiO_2 must fulfill a wide variety of requirements in terms of particle size, morphology, crystallinity, and so forth. In our synthesis, two additional solvothermal reactions were carried out, and the products were synthesized by the same process as that described in the Experimental Section, to get a better understanding of the important influence of cosolvents in the morphology and crystallinity of resulting TiO_2 nanostructures. Analogous to the literature,[21] when no cosolvent was used, an immediate large-scale nucleation and fast crystal growth lead to the formation of TiO_2-B nanosheets, which was confirmed by XRD measurements (the pattern is not shown). The nanosheets have a nonuniform size distribution with a width of about 50−200 nm and a length in the range from 200 nm to 1 μm (Figure 7A). However, by adding ethylenediamine into the reaction system (the total volume of the system does not change), we could obtain a large quantity of ultralong TiO_2−B nanowires. As shown in Figure 7B, the lengths are about a few micrometers and the diameters are about 20−50 nm. According to the corresponding ED pattern, two types of well-crystallized nanostructures reveal different growth directions: the nanosheets are mainly oriented along [110] (Figure 7C), while the nanowires are mainly oriented along [001] (Figure 7D). Grounded on present available experimental evidence, it can be concluded that the cosolvents are important and effective in the nucleation and growth of TiO_2 nanostructures, and they were believed to serve as suitable coordination surfactants to control the anisotropic crystal growth of TiO_2 nuclei. Whenthe reaction conditions are controlled, this strategy might be developed into an effective method for the synthesis of other metal-oxide nanocrystallines.

Conclusions

This study has demonstrated that, by control of the cosolvents, we can selectively fabricate one-dimensional nanostructured TiO_2 of different morphologies, including nanowires and nanotubes, through a facile solvothermal route. Furthermore, this strategy offers an effective method for the preparation of high-quality TiO_2 nanocrystallines and provides a better opportunity for the further investigation of their properties and applications. The obtained nanostructures were found to exhibit a favorable discharge performance as anode materials in the application of lithium-ion batteries, showing great promise for high-power output applications. Therefore, this study is of importance for developing new functional materials, applicable for energy conversion and storage in the future, by the wet-chemistry process.

Acknowledgment. This work was financially supported by the National Natural Science Foundation of China (No. 20435010, No. 20125513, and No. 20575032); a Li Foundation Prize, USA; and a Foundation for the Author of National Excellent Doctoral Dissertation of P. R. China.

IC060477X

(26) Bueno, P. R.; Leite, E. R. *J. Phys. Chem. B* **2003**, *107*, 8868.
(27) Wang, H. Y.; Abe, T.; Maruyama, S.; Iriyama, Y.; Ogumi, Z.; Yoshikawa, K. *Adv. Mater.* **2005**, *17*, 2857.